Luo, S., Diambra, A., & Ibraim, E. (2016). Application of Acoustic Emission on Crushing Monitoring of Individual Soil Particles in Uniaxial Compression Test. In Proceedings of 32nd European Conference on Acoustic Emission Testing: Prague, Czech Republic, September 07-09, 2016. (pp. 305-313). Czech Society for Nondestructive Testing.

APPLICATION OF ACOUSTIC EMISSION ON CRUSHING MONITORING OF INDIVIDUAL SOIL PARTICLES IN UNIAXIAL COMPRESSION TEST

Sha LUO [1], Andrea DIAMBRA [1], Erdin IBRAIM [1]

[1] Department of Civil Engineering, University of Bristol, Senate House, Bristol, BS8 1TH, UK,
Phone: +44 117 928 9000; e-mail: sl13796@bristol.ac.uk, Andrea.Diambra@bristol.ac.uk ,
Erdin.Ibraim@bristol.ac.uk

Abstract

Soil grain breakage has a significant influence on the performance of the geotechnical system. Due to the nature of the underground environment, it is hard to track the soil grain breakage process in both temporal and spatial dimensions. Hence, the use of non-destructive Acoustic Emission (AE) technique to characterise the soil breakage is explored in this work. This study particularly focuses on the individual soil grains, and aims to distinguish the crack formation of the individual silica sand particles with different sizes and shape under uniaxial compression. AE parameters and the signal waveforms at each particle crushing point are analysed. It is found that the AE parameters changing trend match well with the mechanics behaviour in the test, with this, the crack of the silica sand particle could be detected. What is more, in the frequency domain analysis, the difference in the frequency distribution at critical crushing hit within different silica sand test has been found and the possible reason are shown.

Keywords: Acoustic Emission (AE), silica sand particle, crack formation, uniaxial compression, frequency domain analysis

1. Introduction

Acoustic Emission (AE) monitoring technique has been used in various engineering applications mainly for the assessment of damage and failure of brittle materials [1], evaluation of the response of retrofitted reinforced concrete elements [2], detection of the onset and position of failure in fiber reinforced composite materials [3-6], and monitoring of large bridge structures [7]. In geomechanics, pioneering work of Koerner and co-workers [8-11] and more recently [12-15] used the AE technique to assess the stability of soil slopes. Correlations between the characteristics of the acoustic emission in soils subjected to oedometric compression, triaxial testing, cone penetrometer tests, direct shear and deformation properties, including particle crushing have been established by [16-21].

The study of soil breakage phenomena is difficult and complex [22-35]. However, insight into internal mechanisms can firstly be gained through the study of individual soil particles under loading. This study focuses on the use of AE technique for breakage characterisation of discrete silica sand grains under uniaxial compression loading. The discussion of the test results is divided into two parts. In the first part, the observed mechanical response of the silica sand particle during the uniaxial compression test is presented. The relation between the mechanical response and the particle size is also discussed. In the second part, the associated AE parameters which are recorded during the whole uniaxial compression test are analysed. Finally, the statistical analyses of the AE parameters at the crushing point are presented and some correlation between these parameters and the behaviour established.

2. Material

In this work, Leighton Buzzard sand [26-29] which contains about 96% of Si02 has been selected. The size of the particles has been defined in terms of the equivalent area diameter d_a [36] which is the diameter of the circle which has the same area with the projection area of the particle outlet observed in an optical microscope. The equivalent area diameter, d_a, of the silica particles considered in this study is between 1.47 mm and 2.26 mm. Qic-Pic measurements [37] and optical 2D microscope analysis [38] have been used for shape description. The latter measurement technique has been used in this work. The shape descriptors are measured on 2D particle projections of the real 3D particles. These can only be statistically representative if the 2D projections are obtained from particle orientations that are randomly oriented in space [38]. While recognising that such data is not normally attainable using microscopy, in this study, the shape descriptors and d_a for an individual particle have been evaluated based on six microscope images of the particle placed in different positions on the microscope set up as shown in figure 1. Then the shape descriptors have been evaluated from these pictures in Matlab, and the average values recorded. The circularity, $C = (4\pi A)/(P^2)$, irregularity, $IR = d_{imax}/d_{cmin}$, and aspect ratio, $AR = df_{min}/df_{max}$, [36] average values for 60 silica particles are given in table 1, where A and P (figure 2a) are the area and the perimeter of the particle projection, respectively, d_{imax} is the diameter of maximum inscribe circle, d_{cmin} is the diameter of minimum circumscribe, df_{max} is the maximum ferret diameter and df_{min} is the minimum ferret diameter (all defined in figure 2b). According to the suggested circularity classification [41], the mean value of circularity among the 60 silica particle is 0.566, which means this group of silica sands has a low circularity.

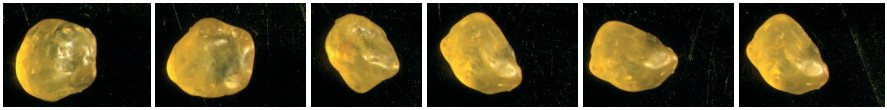

Figure 1. Photos of one silica sand particle in six positions in microscope

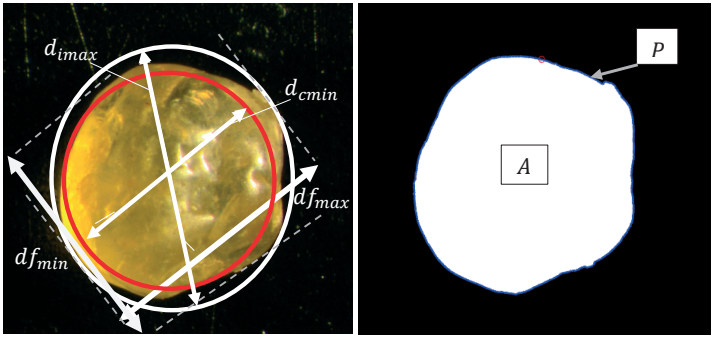

(a) (b)

Figure 2. Photos of silica sand in microscope and Matlab

Table 1. Statistical analysis of shape descriptors of 60 silica particles

	da (mm)	AR	IR	C
Mean	1.889	0.807	0.728	0.566
Variance	0.040	0.006	0.004	0.034
Minimum	1.470	0.560	0.520	0.120
Maximum	2.260	0.960	0.850	0.910

3. Test setting

The uniaxial compression test on individual particles uses a displacement controlled electro-mechanical loading frame (figure 3). Each particle was loaded between two rigid steel platens, of which one is fixed to the loading ram that incorporates an LVDT for vertical displacement measurements and a 5 KN-load cell. The lower platen moves upwards with a speed of 0.05 mm/min.

During the crushing test, two piezoelectric sensors with a bandwidth between 10 kHz and 1 MHz record the acoustic emission signals. The first AE sensor (AE 1), which links to channel 1 of the AE acquisition system, is fixed within the steel base plate, just below the particle at a depth of about 1 cm by means of a mechanical system that ensures a constant holding force (figure 3). The second AE sensor (AE 2), which links to channel 2, is simply placed on the base plate at a distance of about 4 cm from the particle. For both sensors, silicon grease is also used as a coupler. During the crushing test, the resulting vertical force and vertical displacement are recorded, while the AE system allows the acquisition of the acoustic bursts. The typical AE acquisition system setting parameters are listed in table 2.

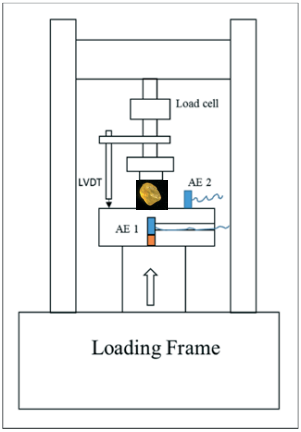

Figure.3. Diagram of loading system

Table 2. Typical settings of the AE acquisition system

Sampling rate	5 MSPS
Recording length	5 K
Preamplifier gain	40 dB
Threshold of detection	40 dB

4. Results & discussions

4.1 Uniaxial compression test

Although the shape and the size of the silica sand particles are not identical, the observed uniaxial compression crushing response follows a similar pattern. A typical force-displacement response obtained during the compression tests is shown in figure 4. In general, no visible cracks are observed during the uniaxial loading test (although for some particles, local crushings possibly of asperities were observed before the final crush, see figure 8), and at some point the sand particle crushes without any warning in a brittle mode. Several small

fragments are generated and ejected in random directions. The maximum force recorded at the crushing point is defined as critical failure force, F_c. For a particle, the tensile stress, σ , developed is F_c/d^2, where d is the particle diameter [32], which in our case, is taken to be d_a. There is some variation of the critical tensile stress among all the tested silica sand particles but overall the data fits well the results obtained by different authors [26] on similar sand (figure 5) which show a decrease of σ with the increase of the size of the silica sand particles. It has also been observed that for some particles, some slight rotation occurred during the loading, and that may explain the change of the force rate evolution observed in force-displacement curves (figure 4). As discussed by [39], in this case, both the normal and the shear forces contribute to the particle crushing and affects the observed force-displacement response.

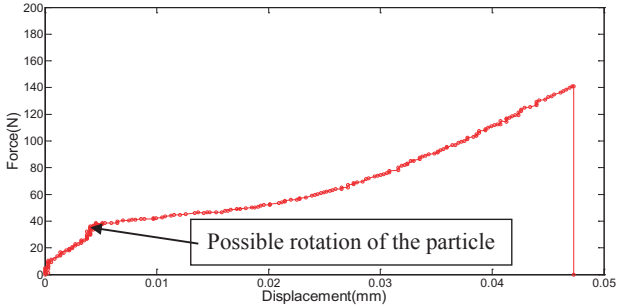

Figure 4. Typical force-displacement line of a silica sand particle under uniaxial compression

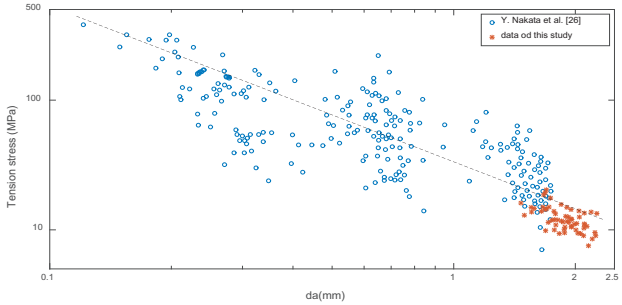

Figure 5. Critical tension stress versus diameter of the silica sand particles (asterisk) and data from Y. Nakata et al [26] on similar sand (hollow circles).

4.2 AE analysis

During the whole uniaxial compression test, the acoustic emission has continuously been recorded by the AE system. We combine the observed mechanical behaviour with the AE parameters during the whole uniaxial compression test. A representation of an AE signal and some associated AE parameters like AE Amplitude, AE Duration, Rise Time, AE Counts and AE Threshold are shown in figure 6. Additional parameters like ASL (Average Signal Level) which is the average of all the amplitudes of the signal can also be deduced. Examples of AE burst signals recorded at the critical crushing point for three particles are shown in figure 7. These three particles have a similar equivalent area diameter, d_a, and the shape descriptors of two of them, designated as silica particle 27 and silica particle 30, are close to the mean value of the 60 silica sand particles, while the shape descriptors like Aspect Ratio and Irregularity of

the silica particle 15 are slightly different compared with the averages of the entire sample. The shape descriptors, critical force and tension stress of the three particles are given in table 3.

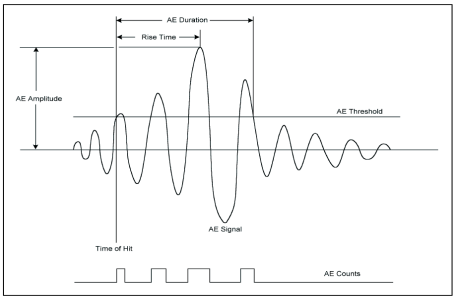

Figure 6. Typical AE burst signal and some associated AE parameters

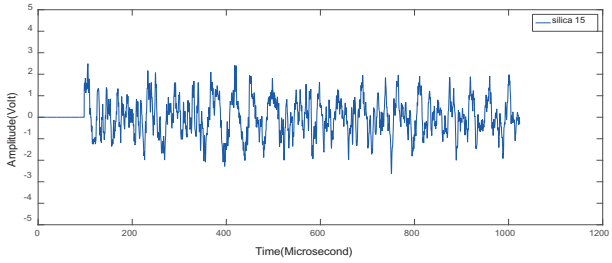

(a)

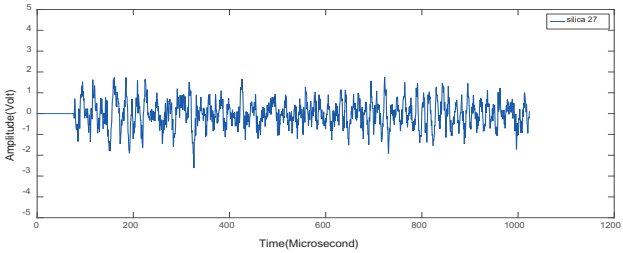

(b)

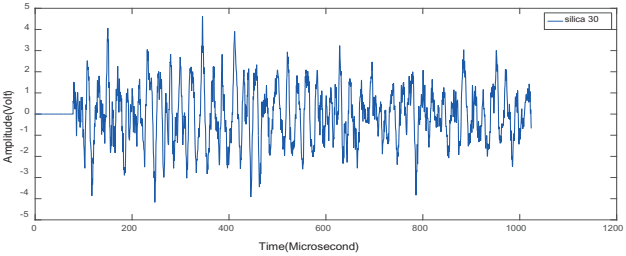

(c)

Figure 7. Original AE burst signal recorded at the critical crushing point for three silica particles: (a) silica 15, (b) silica 27, (c) silica 30

Table 3. Shape descriptors, maximum compression force and corresponding tension stress for the three chosen particles

Particle Name	d_a(mm)	AR	IR	C	Fc (N)	tension stress (MPa)
15	1.87	0.56	0.52	0.72	100.6	28.91
27	1.71	0.84	0.80	0.67	100.6	34.24
30	1.89	0.81	0.73	0.70	113.1	31.56

In the data recorded by the AE system, the Amplitude of the signals at the critical crushing hit reaches 99 dB (figure 8), while the Average Signal Level (ASL) ranges from 20dB to 75dB. The cumulative ASL of all the hits during the tests (figure 9) shows different evolutions for the three tests. It seems that the Amplitude of the recorded signal is a good parameter that may allow the detection of the crushing point of the silica particle, while the value of the ASL and cumulated ASL at the crushing point do not appear to be related to the particle shape and mechanical response information. But the trend of the cumulated ASL matches well with the trend of the axial force, and a drop in the force is well replicated by the cumulative ASL with a sharp jump. When the axial loading is close to the critical crushing force, the slope of the cumulated ASL-time relation increases rapidly. To some degree, this could be used as a way to detect the occurrence of particle crushing.

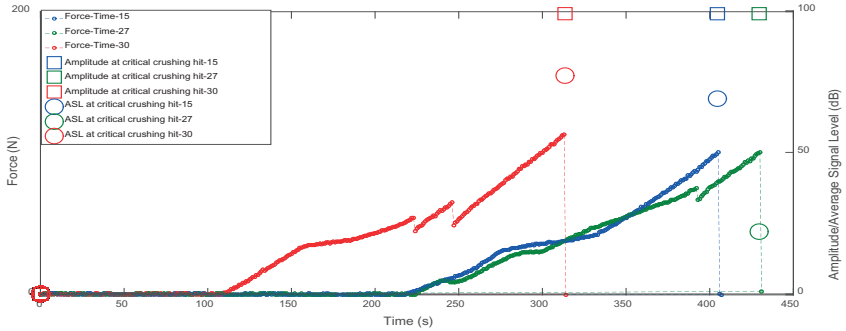

Figure 8. Force-time vs. Amplitude-ASL (Average signal level)at critical crushing hit of the three tests

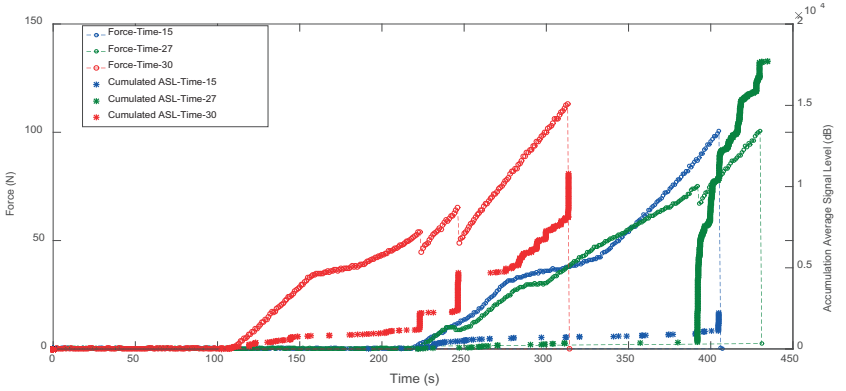

Figure 9. Force-Cumulated Average Signal Level-time diagram of the three tests

4.3 Frequency domain analysis of AE signals

The recorded waveforms at the crushing point (figure 7) are also analyzed in the frequency domain which is based on Welch's power spectral density estimate method [40] and was conducted using Matlab software package. The results for the three particles are shown in figure 10. While the maximum amplitudes correspond to different frequencies for all three particles, the succession of the peak frequencies appears to match well, especially for the silica 27 and silica 30. The peak frequencies for silica 15 are displayed differently and that suggests that the shape of the particle may affect the AE specific signature. In a bulk soil formed by an agglomerate of different particles, this may help discriminate between them if crushing occurs.

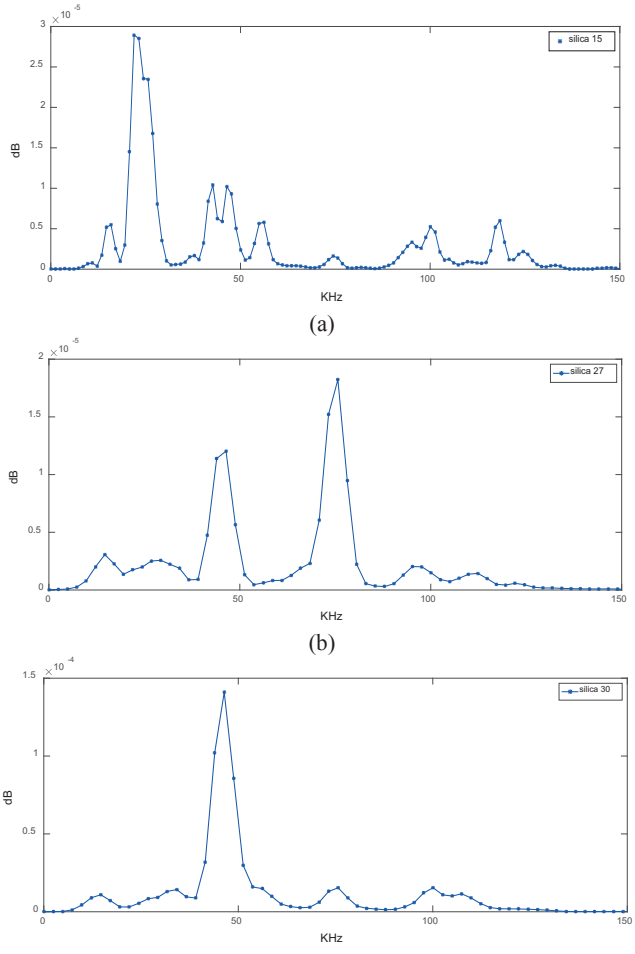

Figure 10. Results of frequency domain analysis: (a) silica sand particle 15, (b) silica sand particle 27, (c) silica sand particle 30.

5. Conclusion

This study focuses on the behaviour of individual silica particles under uniaxial compression loading. The long term objective is the study of crushing phenomena in granular media and the development of non-destructive detection methods for fracture particle characterisation. This study uses the AE technique alongside with mechanical loading of particles and it shows that some AE parameters derived from the analysis of recorded signals can be useful for tracking of the particle fractures as well as crushing identification. Futhermore, the analysis of the recorded signals in the frequency domain appears to be related to the particle shape. Further work is ongoing to estabilsh other criteria for identification of crushing in assemblies of particles. The study is also extended to a large variaty of particles.

References

1. Dai ST, Labuz JF, 'Damage and failure analysis of brittle materials by acoustic emission'. J Mater Civil Eng, Vol. 9(4), pp 200-205, 1997.
2. Yuyama S, Okamoto T, Nagataki S, 'Acoustic emission evaluation of structural integrity in repaired reinforced concrete beams', Material Evaluation, Vol. 52(1), pp 88-90, 1994.
3. Giordano M, Calabro A, Esposito C, D'Amore A, Nicolais L., 'An acoustic- emission characterization of the failure modes in polymer–composite materials', Compos Sci Technol, Vol. 58, pp 1923–1928, 1998.
4. Bohse J., 'Acoustic emission characteristics of micro-failure processes in polymer blends and composites', Compos Sci Technol, Vol. 60, pp 1213–1226, 2000.
5. Huguet S, Godin N, Gaertner R, Salmon L, Villard D. , 'Use of acoustic emission to identify damage modes in glass fibre reinforced polyester', Compos Sci Technol, Vol. 62, pp 1433–1444, 2002.
6. Haselbach W, Lauke B., 'Acoustic emission of debonding between fibre and matrix to evaluate local adhesion', Composite Science Technology, Vol. 63(15), pp 2155–2162, 2003.
7 Shigeishi, M., Colombo, S., Broughton, K.J., Rutledge, H., Batchelor, A.J., Forde, M.C., 'Acoustic emission to assess and monitor the integrity of bridges'. Construction and Building Materials, Vol.15, pp 35-49, 2001.
8. Lord, A.E., Koerner, R.M., 'Acoustic-emission response of dry soils', Journal of Testing and Evaluation 2, pp 159–162, 1974.
9. Lord, A.E., Koerner, R.M., 'Acoustic emissions in soils and their use in assessing earth dam stability', Journal of the Acoustical Society of America, Vol57, pp 516–519, 1975.
10. Koerner, R., Lord, A., McCabe, W., Curran, J., 'Acoustic-emission behavior of granular soils', Journal of the Geotechnical Engineering Division – ASCE, Vol.103, pp 1460–1461, 1976.
11. Koerner, R.M., Lord, A.E., McCabe, W.M., 'Acoustic-emission behavior of cohesive soils', Journal of the Geotechnical Engineering Division – ASCE, Vol.103, pp 837–850, 1977.
12. Chichibu, A., Jo, K., Nakamura, M., Goto, T., Kamata, M., 'Acoustic emission characteristics of unstable slopes', Journal of Acoustic Emission, Vol.8, pp 107–111, 1989.
13. Rouse, C., Styles, P., Wilson, S., 'Microseismic emissions from flow slide-type movements in South Wales', Engineering Geology, Vol.31, pp 91–110, 1991.
14. Dixon, N., Hill, R., Kavanagh, J., 'Acoustic emission monitoring of slope instability: Development of an active waveguide system', Proceedings of the ICE: Geotechnical Engineering, Vol.156, pp 83–95, 2003.
15. Dixon, N., Spriggs, M., 'Quantification of slope displacement rates using acoustic emission monitoring', Canadian Geotechnical Journal, Vol.44, pp 966–976, 2007.
16. Tanimoto, K., Nakamura, J., 'Studies of acoustic emission in soil', Acoustic Emission in Geotechnical Engineering Practice, ASTM STP 750. American Society for Testing and Materials, pp 164–173, 1981.
17. Fernandes, F., Syahrial, A.I., Valdes, J.R., 'Monitoring the oedometric compression of sands with acoustic emissions', Geotechnical Testing Journal, American Society for Testing and Materials 33, pp 410–415, 2010.
18. Wang, Y., Ma, C., Yan, W., 'Characterizing bond breakages in cemented sands using a mems accelerometer', Geotechnical Testing Journal, Vol.32, pp 1–10, 2009.

19. Karner, S.L., Chester, F.M., Kronenberg, A.K., Chester, J.S., 'Subcritical compaction and yielding of granular quartz sand', Tectonophysics Vol.377, pp 357–381, 2003.
20. Villet, W., Mitchell, J., Tringale, P., 'Acoustic emissions generated during the quasi-static cone penetration of soils', Acoustic Emission in Geotechnical Engineering Practice, ASTM STP 750, V. P. Drnevich and R.E. Gray, Eds., American Society for Testing and Materials, pp 175–193, 1981.
21. Aslan, H., and Baykal, G., 'Analysing the crushing of granular materials by sound analysis technique', Journal of testing and Evaluation, Vol. 34, No. 6, 1-7, 2006.
22. Hendron, A. J., 'The behavior of sand in one-dimensional compression', PhD thesis, Univ. of Illinois, Urbana, Ill., pp 50-89, 1963.
23. Terzaghi, K., 'Elastic behavior of sand and clay', *Engrg. News-Rec.,* 95(Dec), pp 987, 1925.
24. Terzaghi, K., and Peck, R. B. 'Soil mechanics in engineering practice'. 1st Ed., John Wiley & Sons, Inc., New York, N.Y., pp 61, 1948.
25 Vesic, A., and Clough, G. W. 'Behavior of granular materials under high stresses.' J. Soil Mech. and Found. Engrg. Div., ASCE, 94(3), pp 661-668, 1968.
26. Nakata, Y., Kato, Y., Hyodo, M., Hyde, F.L. A., and Murata, H. 'One-dimensional compression behaviour of uniformly graded sand related to single particle crushing strength'. Soil and foundation. Vol. 41, No. 2. pp, 39-51, 2001.
27. Nakata, Y., 'Macro and micromechanical behaviour of crushable soil under compression', Geomechanics: pp 585-599, 2005.
28. Nakata, Y., A. F. L. Hyde, M. Hyodo, and H. Murata, 'A probabilistic approach to sand particle crushing in the triaxial test', Geotechnique 49, No. 5, pp 567–583, 1999.
29 McDowell, G. R. and M. D. Bolton, 'On the micromechanics of crushable aggregates', Géotechnique, 48(5), pp 667–679, 1998.
30. McDowell, G. R. and O. Harireche, 'Discrete modelling of soil particle fracture' Technical note. Geotechnique 52, No. 2, pp 131–135, 2002.
31. Mullier, M., U. Tuzun, and O. R. Walton, 'A single-particle friction cell for measuring contact frictional properties of granular materials', Powder Technology 65, pp 61–74, 1991.
32. Jaeger, J. C., 'Failure of rocks under tensile conditions', International Journal of Rock Mechanics and Mining Sciences 4, pp 219–227, 1967.
33. Griffith, A. A., 'Theory of rupture', In Proceedings of the First International Congregation on Applied Mechanics, Delft, pp 55–63, 1924.
34. Hardin, B. O., 'Crushing of Soil Particles', Journal of Geotechnical Engineering 111, No. 10, pp 1177–1192, 1985.
35. Nakata, Y., Kato, Y., Hyodo, M., Hyde, A. F. L., & Murata, H., 'One-dimensional compression behaviour of uniformly graded sand related to single particle crushing strength', Soil and foundation. Vol. 41, No. 2, pp 39-51, 2001.
36. ISO, ISO 9276-6:2008(E), 'Representation of results of particle size analysis — Part 6: Descriptive and quantitative representation of particle shape and morphology', 2008.
37. Cavarretta, I., O'Sullivan, C., Ibraim, E., Martin Lings, M., Hamlin, S., Muir Wood, D., 'Characterization of artificial spherical particles for DEM validation studies'. Particuology 10, pp 209– 220, 2012.
38. Cavarretta, I., O'Sullivan, C., & Coop, M., 'Applying 2D shape analysis techniques to granular materials with 3D particle geometries', In Powders and grains 2009: Proceedings of the 6th international conference on micromechanics of granular media Vol. 1145(1), pp 833–836, 2009.
39. O'Sullivan, C., & Cavarretta, I. 'The mechanics of rigid irregular particles subject to uniaxial compression', Géotechnique, 62(8), pp 681–692, 2012.
40. D.Welch, P., 'The use of fast Fourier transform for the estimation of power spectra: a method based on time averaging over short', IEEE Transactions on Audio and Electroacoustics, Vol. 15, issue 2, pp 70-73, 1967.
41. Blott, S. J., & Pye, K. 'Particle shape: A review and new methods of characterization and classification'. Sedimentology, Vol. *55*(1), pp 31–63, 2008.